Final Technical Report for Research and Development

Spectroscopic Characterization of Microplasmas

Kunihide Tachibana

Professor

Department of Electronic Science and Engineering, Kyoto University,
Kyoto-daigaku Katsura, Nishikyo-ku, Kyoto 615-8510, Japan
E-mail: tatibana@kuee.kyoto-u.ac.jp

Report Documentation Page	Form Approved OMB No. 0704-0188

Public reporting burden for the collection of information is estimated to average 1 hour per response, including the time for reviewing instructions, searching existing data sources, gathering and maintaining the data needed, and completing and reviewing the collection of information. Send comments regarding this burden estimate or any other aspect of this collection of information, including suggestions for reducing this burden, to Washington Headquarters Services, Directorate for Information Operations and Reports, 1215 Jefferson Davis Highway, Suite 1204, Arlington VA 22202-4302. Respondents should be aware that notwithstanding any other provision of law, no person shall be subject to a penalty for failing to comply with a collection of information if it does not display a currently valid OMB control number.

1. REPORT DATE **28 JAN 2008**	2. REPORT TYPE **Final**	3. DATES COVERED **01-09-2006 to 31-08-2007**

4. TITLE AND SUBTITLE **Spectroscopic Characterization of Microplasmas**	5a. CONTRACT NUMBER **FA48690610103**
	5b. GRANT NUMBER
	5c. PROGRAM ELEMENT NUMBER

6. AUTHOR(S) **Kunihide Tachibana**	5d. PROJECT NUMBER
	5e. TASK NUMBER
	5f. WORK UNIT NUMBER

7. PERFORMING ORGANIZATION NAME(S) AND ADDRESS(ES) **Kyoto University,Kyoto-Daigaku Katsura, Nishikyo-ku,Kyoto 615-8510,Japan,NA,615-8510**	8. PERFORMING ORGANIZATION REPORT NUMBER **N/A**

9. SPONSORING/MONITORING AGENCY NAME(S) AND ADDRESS(ES) **AOARD, UNIT 45002, APO, AP, 96337-5002**	10. SPONSOR/MONITOR'S ACRONYM(S) **AOARD-064051**
	11. SPONSOR/MONITOR'S REPORT NUMBER(S)

12. DISTRIBUTION/AVAILABILITY STATEMENT
Approved for public release; distribution unlimited

13. SUPPLEMENTARY NOTES

14. ABSTRACT

We have developed a new type of microplasma integrated device with a fabric structure of insulator-coated thin metal wires. It has been proved that the device can be operated at relatively low voltage of a few kV in air and even under water with the help of hydrogen bubbles produced by electrolysis of water. We have performed spectroscopic measurements for characterizing the properties of microplasmas in a single jet and in an assembly of two-dimensional array for estimating the electron density as well as the reactive species compositions. Although it is clear that more comprehensive research should be continued to grasp the whole image of microplasmas for deriving general scaling laws, we have clarified those high potentiality for the applications to material processing tools and microwave controlling devices.

15. SUBJECT TERMS

16. SECURITY CLASSIFICATION OF:			17. LIMITATION OF ABSTRACT	18. NUMBER OF PAGES	19a. NAME OF RESPONSIBLE PERSON
a. REPORT **unclassified**	b. ABSTRACT **unclassified**	c. THIS PAGE **unclassified**	**Same as Report (SAR)**	**12**	

Standard Form 298 (Rev. 8-98)
Prescribed by ANSI Std Z39-18

Abstract

In the first year of this project, we have investigated the properties of a single microplasma jet driven by a low frequency bipolar pulsed power source in atmospheric pressure He gas flow. From the time resolved measurements by an ICCD camera, it was proved that the plasma plume is ejected like a bullet with a speed of a few tens of km/sec only in the positive phase of the powered electrode on the exit side. The analysis of electric field suggests that a phenomenon similar to the positive corona extension towards the free space through the He gas channel. The laser absorption measurement of metastable He*(2^3S_1) atoms as well as the emission spectra of N_2^+ first positive system proved also a large effect of Penning ionization for the breakdown and the production of OH radicals in the free space.

The performance of this plasma jet has been tested in the CVD of SiO_2 films with TEOS as a source gas. By a linear scan of the substrate a deposition rate up to a few tens of nm/sec was attained with a coaxial-type nozzle structure. Another configuration of crossing the jet with a source gas jet was also tried and the deposition of SiO_2 films was confirmed.

The second part of the research has been devoted to the characterization of microplasma integrated devices for the control of microwaves in the mm to sub-mm wavelength ranges. A discharge device composed of stacked meta-meshes covered with insulating material was used for the purpose to make a planar two-dimensional array of microplasmas. Form the transmittance measurement of mm waves, it was estimated that the average electron density is on the order of 10^{13} cm^{-3}. A peculiar behavior of the reflectance as well as the transmittance was observed from the mesh-electrode assembly, suggesting a metamaterial behavior of the microplasma array due to the surface plasmon-polariton mode.

In the final part, we have developed a new type of microplasma integrated device with a fabric structure of insulator-coated thin metal wires. It has been proved that the device can be operated at relatively low voltage of a few kV in air and even under water with the help of hydrogen bubbles produced by electrolysis of water.

1. Introduction

In recent years, microscale plasmas of μm to mm ranges have been attracting much scientific and technological attention. Those microplasmas generally operated at high pressure regions including atmospheric pressure exhibit characteristics that differ from traditional plasmas operated at lower pressure regions in their plasma parameters and other parameters originating from their small dimensions. When those characteristics are well combined with the inherent properties of plasmas as reactive, light-emissive and conductive/dielectric media, there appear a variety of potential applications for new tools of material syntheses, micromachining, micro chemical analyses as well as photonic devices. In the study of this proposal, by using various spectroscopic techniques, we will characterize the basic plasma properties of microplasmas in two different types: an isolated microplasma jet and a large scale microplasma-integrated device, aiming at applications for material processing and controlling electromagnetic waves. The kinds of gases of our major interest are admixtures of rare-gases (He, Ar, etc.) with small amount of N_2, O_2, and H_2O. However, in the second type source, atmospheric pressure N_2 and air will also be used as the starting gases with some admixed impurities.

2. Experimental Results

2.1. Single microplasma jet
(a) Diagnostics

The structure of a single microplasma jet is shown in Fig. 1(a), in which capacitively coupled ring electrodes are driven by a low-frequency (1~10 kHz) power source, keeping one (upstream) side grounded. When atmospheric pressure He gas is fed through the capillary tube of a few mm inner diameter, a thin plasma jet several centimeters long is blown out into the ambient air. Looking at the temporal image shown in Figs. 1(b) and 1(c) taken by an intensified CCD camera with 50 nsec resolution, it is seen that a lump of plasma is ejected like a bullet with a speed of a few km per second, which is faster than the gas flow speed by about three orders of magnitude. It is also noted that the direction of the jet reverses (toward upstream of the feed gas) when the powered and grounded electrodes are exchanged.

The physical mechanism of this jet has been investigated experimentally and theoretically, and going to be attributed to a mechanism similar to the positive corona extension.[6] It is seen in our measurement of metastable He*(2^3S_1) atoms by a diode-laser absorption method at 1.08 μm, as shown in Fig. 2(a), that the metastable atoms are ejected from the nozzle only in the positive phase of the powered electrode at the exit side. And also the metastable atoms are quickly quenched by N_2 and O_2 molecules in the ambient air. It is also verified by the strong
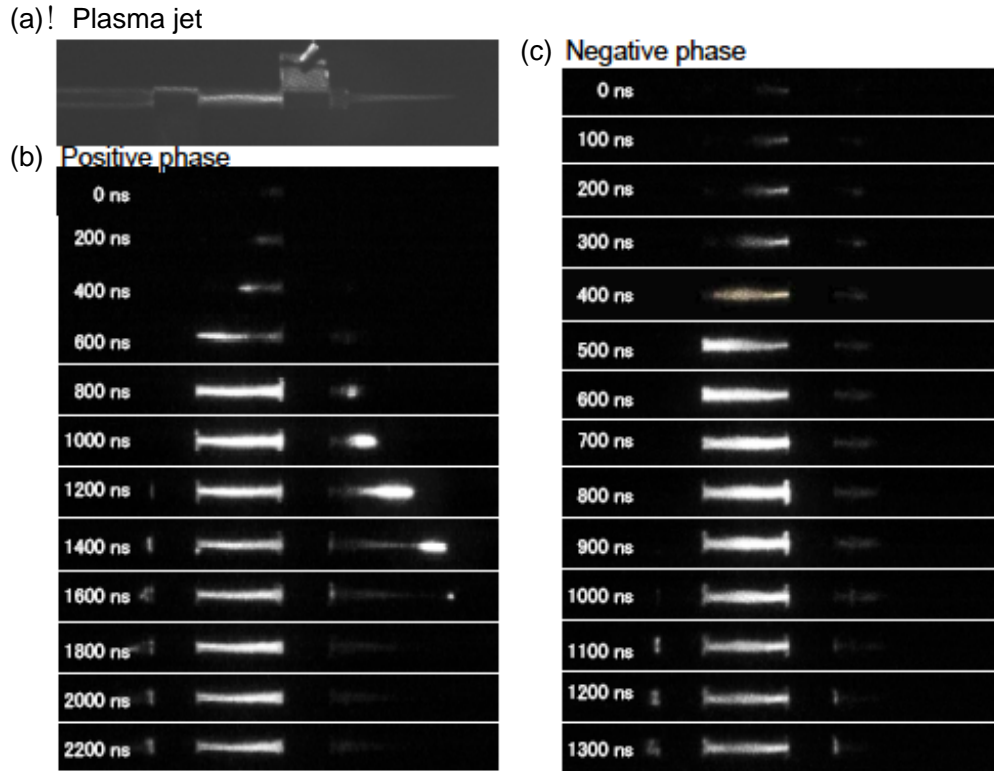
Fig. 1 (a) Microplasma jet and the temporal evolution of the plasma plume in (b) a half-cycle of the positive phase and (c) negative phase of the applied voltage.

1st negative bands of N_2^+ spectra produced via Penning ionization collisions of N_2 molecules with He*(2^3S_1) atoms. Figures 2(b) and 2(c) show the temporal behaviors of the emissions from N_2*, N_2^+ and OH* molecules as well as O* and He* atoms observed at a fixed position (5 mm downstream) through a series of pinholes. It is interesting to see that only the emission from OH*, O*, and H* radicals last for a fairly long time probably due to their production mechanisms, which need to be investigated further.

Another interesting finding in this research was in a cross flow experiment of the microplasma jet with a gas jet. The experimental situation is shown in Fig. 3(a); the same glass tubes were used both for the plasma jet and the gas jet, but there were no electrodes wound on the gas jet. It was surprising to see the discharge was ignited in the gas flow crossing with the plasma jet as shown in Fig. 3(b). This phenomenon was only observed when He or Ne gas is used in the gas jet, suggesting that the corona-like discharge was triggered at the crossing point and propagating along the gas channel.

(b) Applications

We are searching for applications of the microplasma jet in material processing.[2] One example we can show here is the plasma chemical vapor deposition (CVD) of SiO_2 film by
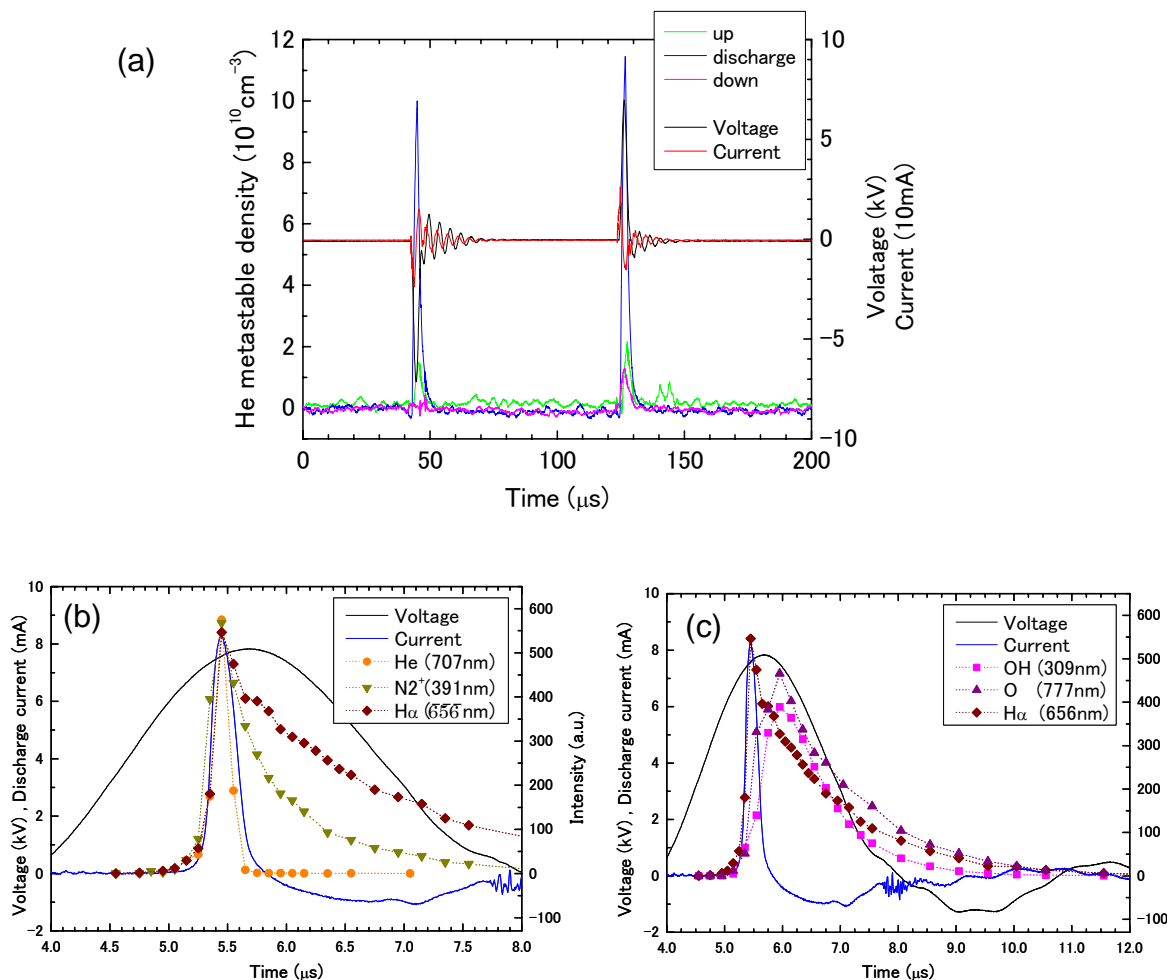
Fig. 2 (a) Temporal behavior of metastable He*(2^3S_1) atoms with the applied volatege and current waveforms, and (b) and (c) those of emission spectral intensities from He, N_2^+, H_α, OH and O excited species.

using tetra-ethyl-organo-silicate (TEOS) as a source material. In the first trial, we used a coaxial nozzle structure as shown in Fig 4(a); the vapor of TEOS admixed with He was fed through the central metal pipe of 1/8" outer diameter and the additional He gas flow was fed through the outer glass tube for sustaining the discharge of the plasma jet. The substrate was set at several distances from the exit of the jet and it was linearly scanned with a speed of 1 cm/min. Obtained results of the deposition rate are shown in Fig. 4(b) as a function of the discharge driving frequency at two different substrate distances. A fairly high deposition rate of about 50 nm/sec was attained and the deposited film had approximately stoichiometryic composition of Si and O with a trace of C as an impurity. We are trying to increase the deposition rate up to 100 nm/sec on a flattened sheet glass fiber as the linear (1D) substrate aiming at the application to the fiber OLED lamp. For the purpose, the diagnostics of the gas flows and the reactive species will be necessary to optimize the deposition reaction.
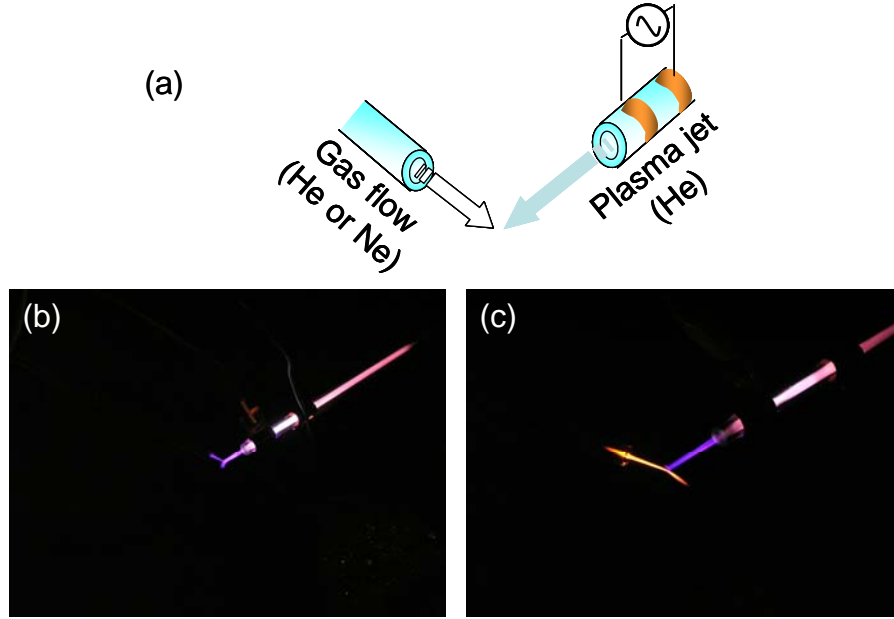
Fig. 3 (a) Crossed configuration of a microplasma jet with a gas flow of He or Ne
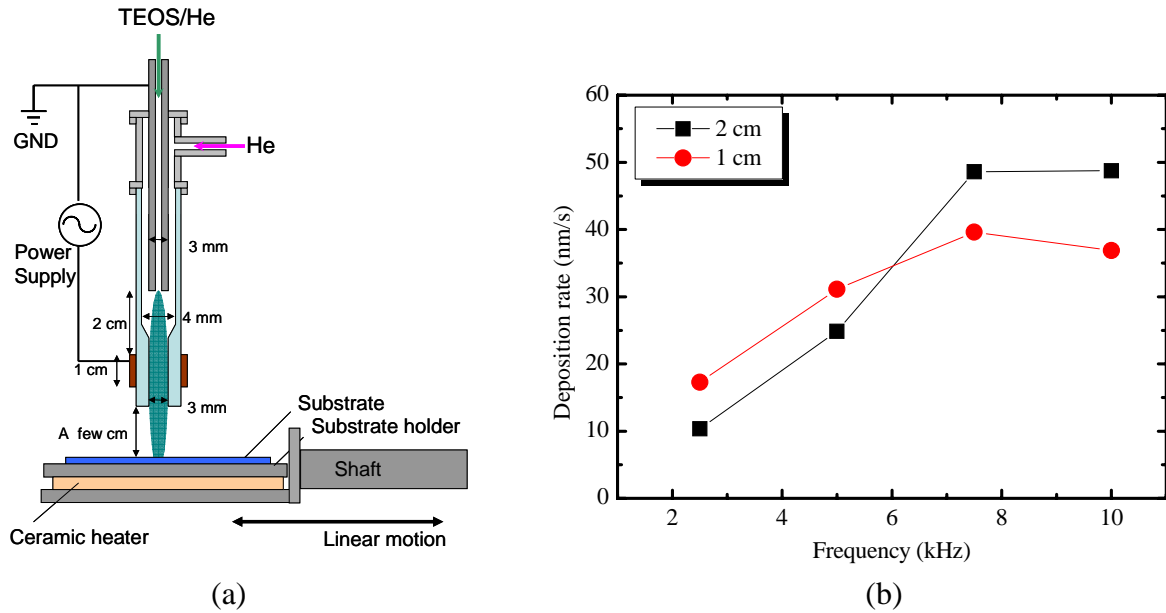and the discharge images with (b) He flow and (c) Ne flow.

Fig. 4 Experimental arrangement for the CVD of SiO₂ films with a coaxial flow of TEOS
and (b) the obtained deposition rate as a function of the discharge frequency.

2.2. Integrated microplasma devices

(a) Diagnostics

We have been studying functional properties created by integration of microplasmas such as a plasma photonic crystal: an artificial dielectric matter. In this experiment, a two-dimensional array composed of microplasma columns were generated by a pulsed DC
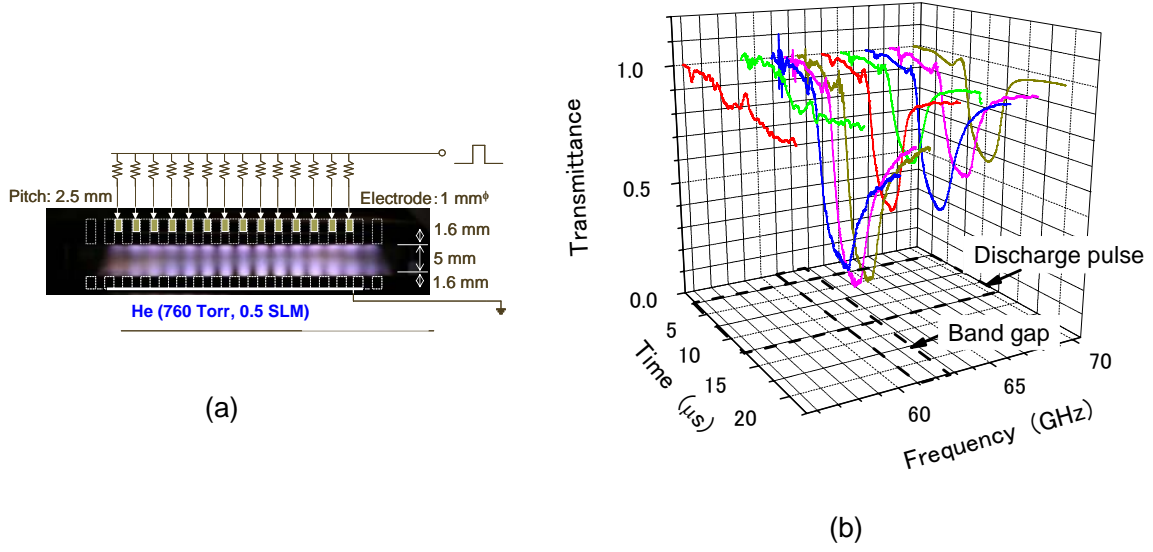
Fig. 5 (a) Structure of 2D microplasma array and (b) temporal evolutions of transmittance at several values of millimetre wave frequency. Plasma columns 1.0 mm diameter are arranged in two-dimensional square lattice with lattice constant $a = 2.5$ mm.

discharge using 17×30 arrays of capillary electrodes with series resistors as shown in Fig. 5(a). Thus, the produced plasma columns were surrounded by the ambient gas of He at 200 Torr with flow rate of 2.0 litter per minute transversely through the plasma columns. Figure 5(b) shows an experimental result about the time evolution of transmittance signals at several values of $\omega/2\pi$. Here we note that the electron density was estimated to be $n_e \sim 1 \times 10^{13}$ cm^{-3} as mentioned later, and so the first band gap in the Γ-X direction was located at $\omega/2\pi \sim 62$ GHz or $\omega a/2\pi c \sim 0.50$. A clear drop of the transmittance signal was detected at 60 - 63 GHz, and it extinguished within 5 μs with the decay of plasmas, which indicated a rapid dynamic switching capability of this phenomenon. The transmittance signal in the band gap attenuated down to 0.18 of its initial value, and this attenuation ratio increased either with the number of rows of the plasma columns in the traveling direction or with the electron density n_e. For instance, when n_e increases up to about 2×10^{13} cm^{-3}, the signal attenuation is estimated to reach 0.005 of its initial value from a numerical calculation based on a super cell method.

From another viewpoint, this phenomenon is useful for the estimation of n_e in each plasma column in the following manner. The attenuation level varies with n_e at a fixed number of rows of the plasma columns. Then if we estimate the transmittance as a function of n_e, we have different curves depending on the number of rows N as a parameter. Such a result is shown in Fig. 6 calculated at $N = 17$ and 30. Whereas, the measured values of the transmittance at those values of N lie at the levels of dashed lines. As the result, we can
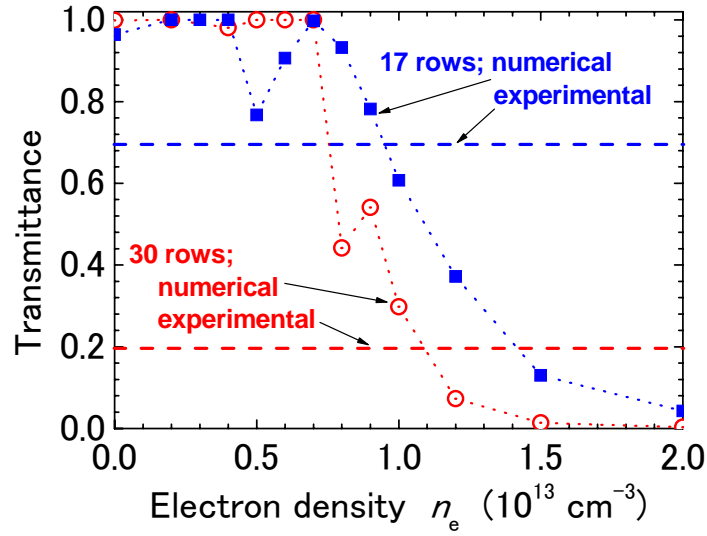
Fig. 6 Numerical results of transmittance calculated as a function of electron density and number of rows of plasma column N using a super cell method by the finite difference method. Inset horizontal lines are experimental results with two different values of N in the alignment.

determine the average value of n_e in a plasma column as $(1.0 \pm 0.2) \times 10^{13}\,cm^{-3}$, which leads to the agreement of experimental and calculated data in both cases simultaneously.

The cases described above are examples of the transmittance characteristics in the frequency range higher than $\omega_{pe}/2\pi$ where plasma is working as dielectric matter. We will expand the frequency toward the lower range in the following experimental situations.

(b) Analysis of metamaterial properties

Previously, we studied the microwave transmittance characteristics through microplasmas generated in holes of double-layered metal-mesh plates covered with dielectric layers, and used the results in the analysis of n_e with the help of a collisional Drude model,[8] as was done above in a different configuration with microplasma columns. However, the frequency dependence was not fully understood in detail. The structure of our stacked metal-meshes resembles the configuration used in the recent study on the abnormal transmission of THz waves. Therefore, in this report we try to investigate further the abnormal transmission through a perforated plate using the structure with 1.8 mm x 1.6 mm openings at a pitch of 2.5 mm x 2.1 mm, and see the additional effects of the presence of microplasmas in the perforated area.[1,7] Since the dielectric layer (Al_2O_3) covering the metal plates was about 0.15 mm thick, the effective area for the discharge in a hole was 1.5 mm x 1.3 mm.
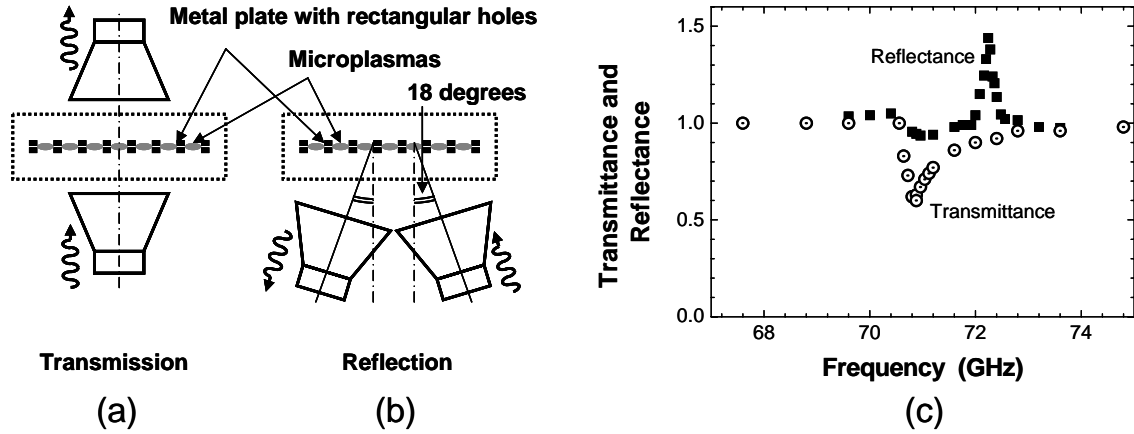
Fig. 7 Experimental arrangements for (a) transmittance and (b) reflection measurements and (c) the measured signals as a function of the transmitted microwave frequency normalized to the values without plasma.

Figure 7(a) shows the experimental setup for the transmittance measurement with the stacked metal-mesh plates covered with insulating films, where microplasmas are generated inside the holes in a scheme of dielectric barrier discharge by applying square-shaped bipolarvoltage (5 μs in width and 5 kHz in repetition) between the two metal plates. Pyramidal horn antennas were used as a transmitter and a receiver, and the frequency of the microwave was swept from 50 to 75 GHz. Figure 7(b) shows the setup for the reflectance measurement with an incidence angle of 18 degrees. We confirmed that direct coupling between two antennas were negligibly small, and almost all part of the detected signals was due to the reflected component from the perforated metal-plate assembly. In both cases, the electric field of the transmitting waves were set parallel to the longer side of the rectangular holes by selecting the angle of the pyramidal horn antennas. The discharge operation at atmospheric pressure of He with flow rate of 1.9 litter per minute through the area of 50 mm x 50 mm. It is seen that microplasmas are confined inside the holes and attaching on the side walls along the direction of the shorter side; microplasmas do not occupy the entire opening area of the holes.

Figure 7(c) shows the results of the transmittance and reflectance signals as a function of the frequency given in the ratio between the values with and without discharge. Abnormal responses from the plasmas were observed in the narrow frequency region from 70 to 74 GHz. The transmittance was suppressed by about 30% of its initial level. If this attenuation of the transmittance is only due to the elastic collisions of electrons (Ohmic loss), the attenuation rate remains at a level of a few percent, as in our previously reported results in non resonant conditions (not at a specific frequency showing abnormal behavior). On the contrary, the
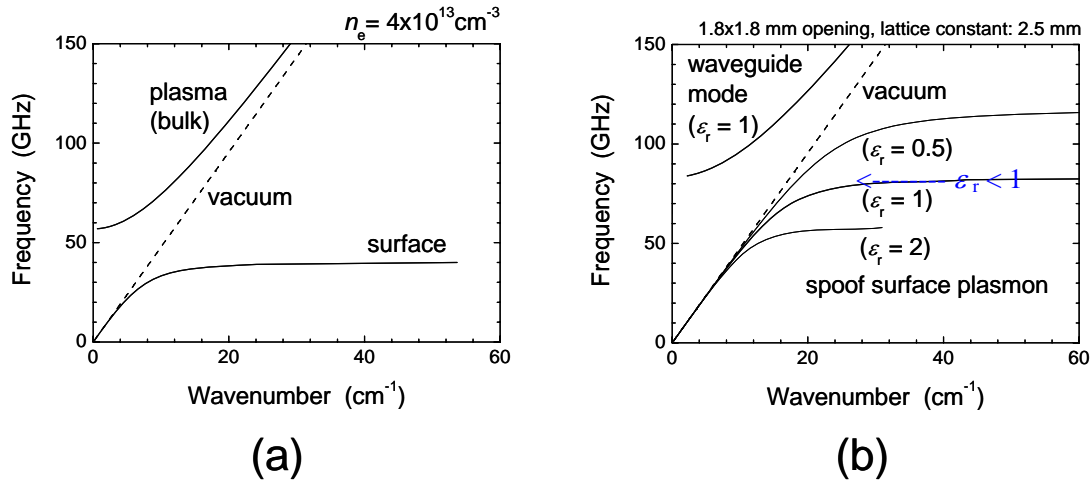
Fig. 8 Dispersion relation of bulk plasma with $n_e = 4 \times 10^{13}\,\text{cm}^{-3}$ including the surface wave mode.

reflectance was enhanced by about 40%, although the observed frequencies where the suppression and the enhancement have peaks are not exactly the same. The reason of this inconsistency is not exactly comprehended at this moment, but may be attributed to the difference in the incident angles. In any case, these experimental results indicate that a part of the incident power of the electromagnetic waves is reflected by the presence of the microplasmas and the transmittance is suppressed by the same amount.

One of the plausible explanations about this abnormal phenomenon will be described in the following by starting from the Pendry's theory.[7] Figure 8(a) shows the dispersion relation of bulk plasma with $n_e = 4 \times 10^{13}\,\text{cm}^{-3}$ including the surface wave mode. We note that the surface wave mode was calculated in the situation where medium with the dielectric constant ε_r of unity is attaching on the surface of the plasma with step density profile. From this figure, a plasma can behave as a medium with negative ε_r (below $\omega_{pe}/2\pi$ in the bulk), positive ε_r from 0 to 1 (above $\omega_{pe}/2\pi$), and positive ε_r from 1 to infinity (below the resonance frequency of the surface wave mode). Figure 8(b) demonstrates the dispersion relation of the spoof surface plasmon plaritons with several different dielectric constants calculated with the parameters in our perforated metal plates. First of all, it should be noted that in the case of ε_r =1 a resonance frequency appears that is very close to the frequency range of the abnormal responses shown in Fig. 7(c).

If the frequency of waves is in the range above $\omega_{pe}/2\pi$ of microplasmas, and consequently ε_r in the holes filled with microplasmas becomes smaller, the working point at this frequency along the dispersion relation will get apart from the resonance (or wave number becomes smaller as shown in Fig 8(b)). The abnormal transmission through both sides of perforated

metal should become smaller as the working point gets apart from the resonance. This situation consists well with the experimental observation in Fig. 7(c).

2.3. New configuration of microplasma integration

As a new type of the integration schemes, we have been trying to use a fabric structure of insulator-coated thin metal wires as shown in Fig. 9.[4] The stricture is very simple and easy to construct in addition to the benefit of flexibility. The discharge can be obtained at relatively low voltage even in air and, therefore, useful for applications such as surface cleaning and sterilization. A noticeable new result we can show here is the discharge generated under water. In the experiment we used a fabric electrode assembly composed of naked metal wires as the
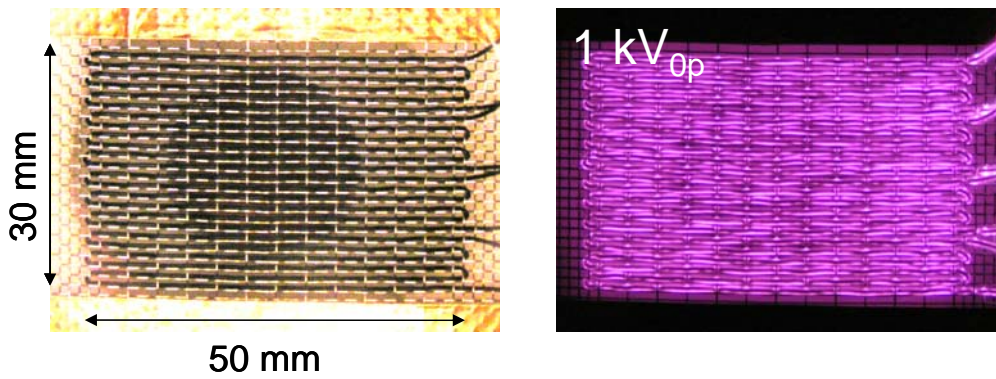

Fig. 9 (a) Example of an electrode assembly with fabric structure and (b) the discharge image in air.
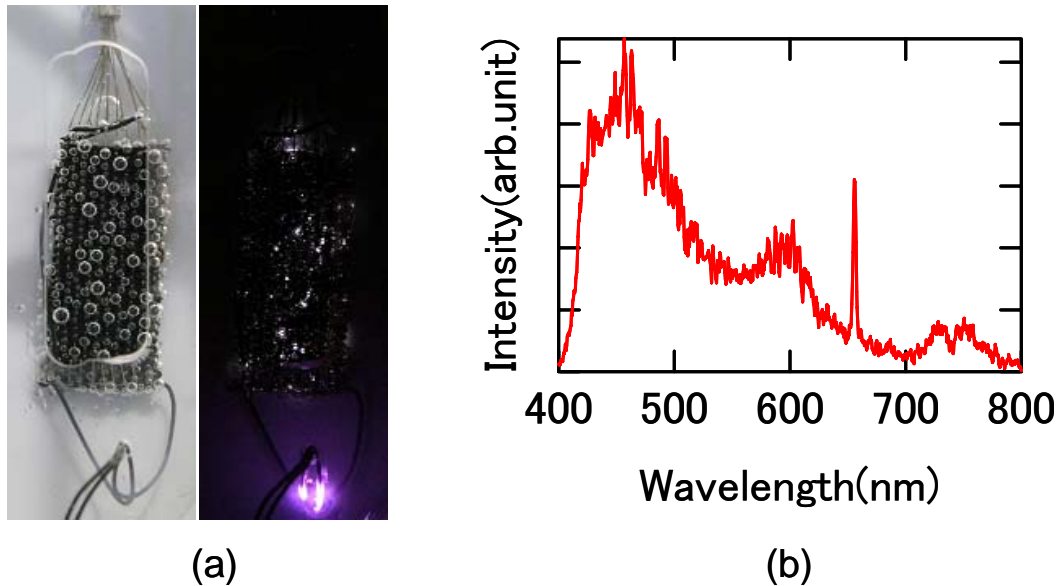

Fig. 10 (a) Electrode assembly with hydrogen bubbles and the discharge image, and (b) the observed spectra in the discharge.

weft and dielectric coated metal wires as the weft. The third metal electrode was placed at a distance with a DC power source connected to the fabric electrode assembly. As easily imagined, hydrogen bubbles were produced on the surface of the fabric electrode by the electrolysis of water, and then the discharge within the bubbles were observed as shown in Fig. 10(a). In the observed spectra shown in Fig. 10(b) emissions from H_2* molecules and H* atoms are seen.   In general, a high voltage source with narrow pulse width of ns order is used to obtain the breakdown in water, but in our case with hydrogen bubbles the discharge voltage was as low as a few kV. This scheme may be very useful for the environmental and biomedical applications. For those purposes, the spectroscopic characterization of the microplasmas is also needed as future objective.

3. Summary of Results and Conclusions

On a low frequency driven single microplasma jet, we have observed the spatiotemporal development of the plasma plume. The result is consistent with the behaviors of $He(2^3S_1)$ metastable atoms and the excited species such as N_2^+, N_2*, OH*, H* and O*, showing a large contribution of Penning ionization for the discharge and the production of reactive species. We are now continuing a laser induced fluorescent measurement on the microplasma jet for a further analysis of the discharge mechanisms. In the measurement the line profile of N_2^+ spectra of the first negative band at around 391.4 nm is analyzed for the identification of the velocity of ions in the plasma bullet. As the result, we hope we can clarify the ionization mechanisms in the bullet whether it is really due to the corona expansion or not.

As for the electron density n_e of plasma column in the assembly of microplasmas, we have performed the microwave transmittance measurement to obtain an overall average value and shown the effectiveness as described above. However, in the measurement we have assumed the collision frequency ν_{me} appropriately from the reported cross section data. Alternatively, both n_e and ν_{me} can be obtained simultaneously if we can measure both the transmittance and the phase shift of the transmitting microwaves. This kind of measurement becomes possible in a terahertz time-domain spectroscopy in which a Fourier-transform method is employed in the frequency domain. We hope we can present a preliminary result soon later.[3] On the other hand, we have also been preparing a laser interferometric method for the measurement of n_e by using an infrared CO_2 laser at 10.6 μnm combined with a heterodyne technique. By this method we can measure the cross sectional distribution of n_e in an individual plasma column with a spatial resolution of 0.1 mm order.

In conclusion, we have performed spectroscopic measurements for characterizing the properties of microplasmas in a single jet and in an assembly of two-dimensional array for estimating the electron density as well as the reactive species compositions. Although it is clear that more comprehensive research should be continued to grasp the whole image of

microplasmas for deriving general scaling lows, we have clarified those high potentiality for the applications to material processing tools and microwave controlling devices.

4. Presentations and Publications

The results of present research have been partially presented or scheduled to be presented at several international conferences. As for the publication in scientific journals, it will be followed up within a year except one paper, in which a part of the results on the metamaterial properties of microplasmas is scheduled for the publication.

(a) Presentations

1) K. Tachibana and O. Sakai: *"Metamaterials composed of artificial array of microplasmas and the diagnostics"*, 34th European Physical Society Conference on Plasma Physics, Warsaw, July, 2007.

2) Y. Ito, K. Urabe, M. Kubo and K. Tachibana: *"Study of plasma jet using coaxial dielectric barrier discharges at atmospheric pressure"*, 18th International Symposium on Plasma Chemistry, Kyoto, August, 2007.

3) H. Nakanishi, D.-S. Lee, O. Sakai and K. Tachibana: *"Electron density and collisional frequency in plasma with terahertz time-domain spectroscopy"*, 18th International Symposium on Plasma Chemistry, Kyoto, August, 2007.

4) O. Sakai, T. Shirafuj and K. Tachibana: *"Atmospheric pressure discharge ignited on flexible electrodes of fabric structure"*, 18th International Symposium on Plasma Chemistry, Kyoto, August, 2007.

5) M. Kimura, T. Shirafuji, O. Sakai and K. Tachibana: *"Discharge characteristics of the plasma in liquid media"*, 18th International Symposium on Plasma Chemistry, Kyoto, August, 2007.

6) B. Sands, B. Ganguly and K. Tachibana: *"Spatio-temporal behavior of dielectric capillary atmospheric gas mixture plasma jet"*, 60th Annual Gaseous Electronics Conference, Arlington, VA, October, 2007 (to be presented).

(b) Publications

1) O. Sakai, T. Sakaguchi, T. Naito, D.-S. Lee and K. Tachibana: Characterization of metamaterials composed of microplasma arrays", Plasma Physics and Controlled Fusion, **49** (2007) to be published.

2) O. Sakai and K. Tachibana: *"Properties of Electromagnetic Wave Propagation Emerging in Two-Dimensional Periodic Plasma Structures"*, IEEE Transactions on Plasma Science, **35** (2007) in press.